



Biological: Full-length

Ultrastructure of *Felis catus* whole fetus (Fcfw-4) cell culture following infection with feline coronavirus

Amer Alazawy¹, Siti-Suri Arshad^{1,*}, Mohd-Hair Bejo¹,
Abdul-Rahman Omar¹, Tengku-Azmi Tengku Ibrahim²,
Saeed Sharif¹, Faruku Bande¹ and Kamarudin Awang-Isa¹

¹Department of Veterinary Pathology and Microbiology, Universiti Putra Malaysia, 43400 UPM Serdang, Selangor, Malaysia and ²Department of Veterinary Preclinical Sciences, Faculty of Veterinary Medicine, Universiti Putra Malaysia, 43400 UPM Serdang, Selangor, Malaysia

*To whom correspondence should be addressed. E-mail: suri@putra.upm.edu.my

Abstract Feline coronavirus (FCoV) consists of two biotypes based on their growth in cell culture and their antigenicity. Infections with FCoV are highly prevalent in the cat population worldwide. In this study, *Felis catus* whole fetus (Fcfw-4) cell culture was infected with FCoV UPM11C/08. Virus multiplication in cell culture was monitored and examined under the transmission electron microscope. The virus particles revealed the characteristic morphology of feline FCoV represented by envelope viruses surrounded by peplomers. Virus attachment and entry into the cell occurred 15 h post-infection (pi), and the myriad of virus particles were observed both extracellularly and intracellularly after 48 h pi. Thereafter, intracellular virus particles were observed to be present in vacuoles or present freely in the cytoplasm.

Keywords feline coronavirus, *Felis catus* whole fetus (Fcfw-4), transmission electron microscopy, vacuoles

Received 17 November 2010, accepted 17 April 2011

Introduction

Feline coronavirus (FCoV) is known to be a prevalent infection in cat populations, with particularly high prevalence in catteries and multiple-cat households [1–3]. The genome is characterized as an RNA virus under the family *Coronaviridae*, order *Nidovirales*

[4,5]. It was first recognized in the 1950s as a specific disease of cats [6] and its first occurrence was in Malaysia in 1981 [7]. Two pathotypes of coronaviruses were described in cats: feline infectious peritonitis virus (FIPV) and feline enteric coronavirus (FECV). These FCoVs are spread worldwide and infect cats and other members of the *Felidae* family. FECV is the common form of FCoV, which causes right from asymptomatic infection to severe

enteritis and can be transmitted in nature between cat populations [3, 8]. Unlike FECV disease, FIP is an immune-mediated progressive polyserositis and pyogranulomatosis. It is the most important cause of death of infectious origin in cats worldwide, affecting both domestic and wild *felids* [6, 8]. Circulating antibodies against FCoV are found in 90–100% of the cats living in catteries or multiple-cat households and up to 50% of solitary cats house. However, only 1–5% of the seropositive cats eventually came down with FIP [9–11].

Both FECV and FIPV are further subdivided into two different serotypes I and II based on their antigenic relationship to canine coronavirus, neutralization reactivity with S-protein-specific mAbs, sequence analysis of the S protein gene and growth

ability *in vitro*. While serotype I grows poorly in cell cultures, serotype II can grow well in many cell line [12–14]. FECV is more tropic for mature apical epithelium of the bowel, whereas FIPV infects blood monocytes and spreads systemically [8, 12, 15]. Most coronaviruses will grow only in cells derived from the natural host animal or in cells from a closely related species. FCoV serotype I strain is difficult to grow *in vitro*; hence studies on these viruses have been limited in view of their fastidious growth in cell culture. On the other hand, serotype II FCoV could be propagated more readily in cell cultures. Growth of FCoV in a continuous feline cell line of *Felis catus* whole fetus-4 (Fcfw-4), which possesses the properties of macrophages [16–18], was characterized by cytopathic changes and giant cell formation. After binding itself to specific receptor of infected cells, the virus enters the latter by fusion either with the plasma membrane or the endosome. The viral nucleocapsid is released into the cytoplasm of infected cells to become available for translation and transcription [14, 19].

FCoV has been described as large pleomorphic particles with numerous spike-like projections extending from their envelope. Particle measurements ranged from 75 to 150 nm in diameter. Surface projections have been observed to vary in size and shape, reported between 12 and 25 nm in length [8, 20, 21]. Thus, the aim of this study was to describe the physical properties of FCoV UPM11C/08 isolates and the ultrastructure of Fcfw-4 cell line following infection with this local isolate of FCoV.

Materials and methods

Virus

A prototype of local isolate FCoV designated as UPM11C/08 was used in the study. The virus was isolated from a cat presented at the University Veterinary Hospital, Universiti Putra Malaysia (UVH-UPM) with effusive-form FIP. Ascitic fluid was obtained from the cat and screened for FCoV with reverse transcriptase polymerase chain reaction assay using primers targeting the untranslated region of 3'UTR [22]. The sample was adapted and propagated in Fcfw-4 cell culture until characteristic cytopathic effect (CPE) was observed and

stored at -20°C (Sanyo, Malaysia) for further purification by sucrose gradient method. This isolate was confirmed as type 1 FCoV (GenBank, HM 628778).

Cell culture

Fcfw-4 cell culture was obtained commercially (ATCC CRL-2787) and maintained in Eagle's minimum essential medium, supplemented with 15% heat-inactivated fetal bovine serum (FBS) (Gibco, UK), 100 IU of penicillin/ml, 100 μg of streptomycin/ml and 2.5 μg of amphotericin/ml. Cultures were maintained in a humidified incubator at 37°C with 5% CO_2 (Galaxy, UK).

Virus inoculation

A total of 20 flasks (150 cm^2) (Nunc, Denmark) containing confluent monolayer of 3-day-old Fcfw-4 cells were infected with 100 μl of purified virus stock for each flask, where five flasks were kept as control receiving only saline. All infected and control flasks were incubated at 37°C for 1 h to allow virus adsorption before adding the maintenance media containing 2% FBS. The cells were further incubated and examined daily for CPE. For transmission electron microscopy (TEM) analysis, two infected flasks and one control flask were removed consecutively at 6, 10, 15, 24 and 48 h post-infection (pi).

Virus purification

The virus stock was purified by sucrose gradient for the purpose of ultrastructural studies and negative staining analysis. Briefly, infected culture exhibiting 80% CPE was freeze-thawed thrice, pooled and centrifuged at $6000 \times g$ for 30 min (Hettich, Germany). The supernatant was subjected to ultracentrifugation at $25\,000 \times g$ for 3 h at 4°C (Beckman, USA). The resultant pellets were resuspended in 1 ml of Tris NaCl EDTA (TNE) buffer (0.05 M Tris, 0.001 M EDTA, 0.15 M NaCl) and gently layered over a 20–50% sucrose density gradient and centrifuged at $120\,000 \times g$ for 8 h. The resultant virus band was pooled and diluted with an equal volume of TNE buffer and pelleted again by centrifugation at $120\,000 \times g$ for 60 min. The purified virus was resuspended in the TNE buffer and stored at -70°C (Rifco, Germany) until further use.

Negative contrast electron microscopy

The purified virus was examined for negative contrast electron microscopy (NCEM) according to the method of Gelderblom *et al.* [23]. Briefly, a drop of purified virus was placed on a parafilm and a carbon-coated formvar grid (Van Loenen Instrument, The Netherlands) was floated on the virus drop for 7 min. The grid was removed and excess liquid was blotted away and fixed with a drop of 2% phosphotungstic acid (Sigma, USA) for 5 min. The grid was air-dried before examination under TEM (Hitachi H7100, Japan) at an accelerated voltage of 75 kV.

Transmission electron microscope

Control and infected Fcwf-4 cells were processed for TEM according to the method of Hayat [24] with some modification. Cell cultures were scraped from the flasks, washed thrice with phosphate-buffered saline and centrifuged at $6000 \times g$ for 30 min. The pellets were fixed in 4% glutaraldehyde with 0.1 M sodium cacodylate buffer for 4–6 h at 4°C, washed with 0.1 M sodium cacodylate buffer, postfixed with 1% aqueous osmium tetroxide for 2 h and again rinsed in 0.1 M sodium cacodylate buffer. Following addition of FBS, pellets were dehydrated in a graded series of dilutions of acetone in distilled water (35, 50, 75 and 95%) for 10 min each, followed by three changes of absolute acetone for 15 min each. Pelleted samples were initially infiltrated with a 50:50 mixture of resin and acetone and subsequently embedded in resin and polymerized in an oven at 60°C overnight (Mettler, Germany). Ultrathin sections on a copper grid were stained with uranyl acetate and lead citrate [25]. The preparations were examined under TEM.

Results

Negative contrast electron microscopy

NCEM of purified virus revealed the characteristic features of a coronavirus. The virion exhibited slight pleomorphic features, spherical to oval shape with a diameter ranging from 75 to 150 nm. The morphological features of FCoV UPM11C/08 isolates were similar to those of other members of the family *Coronaviridae*. Their corona demonstrated

the long petal-shaped surface projections up to 21 nm long (Fig. 1).

Transmission electron microscopy

Infected Fcwf-4 cell culture showed the presence of typical FCoV particles. At 15 h pi, the virus particles were observed extracellular and by 48 h pi, the virus particles were found to be present at both intracellular and extracellular. In the extracellular compartment, the virus particles were spherical measuring between 55 and 69 nm in diameter, with spike-like electron-dense envelope. Numerous virus particles were closely apposed to the host cell plasma membrane (Fig. 2). At the same time, virus particles were observed to penetrate the cell by invaginating the plasma membrane. It carried into the cytoplasm part of the cell membrane that it invaginated to form vesicles (Fig. 3). Virus-like particles which morphologically resembled those of extracellular virus particles were present in vacuoles of different sizes, with smaller vacuoles containing 1–4 particles, while larger ones contained 5–24 virus particles (Fig. 4). In addition to the rough spike-like electron-dense virus-like particles, there were also particles which were larger in diameter ranging from 69 to 149 nm with distinct smooth electron-opaque surfaces (Fig. 5). The vacuole containing these particles was distinctly more rounded, firm with a thicker membrane. In many instances, the vacuole membranes were seen to be no longer intact leading to spillage of virus particles into the cytoplasmic matrix (Fig. 6). In this context, the virus particles were either in a form of aggregations in the cytoplasmic matrix or occur singly in a vesicle of the Golgi apparatus or within the endoplasmic reticulum (Fig. 7).

Discussion

This study reports a new insight into the ultrastructure of Fcwf-4 cell culture following an infection with FCoV. The prototype FCoV UPM11C/08 was isolated from ascitic fluid of a cat diagnosed as effusive form of FIP. The purified FCoV possesses the characteristic of coronavirus with the diameter and peplomer sizes within the range of published data [20, 21, 26]. Upon virus replication at 15 h pi, the virus particles were detected extracellularly in

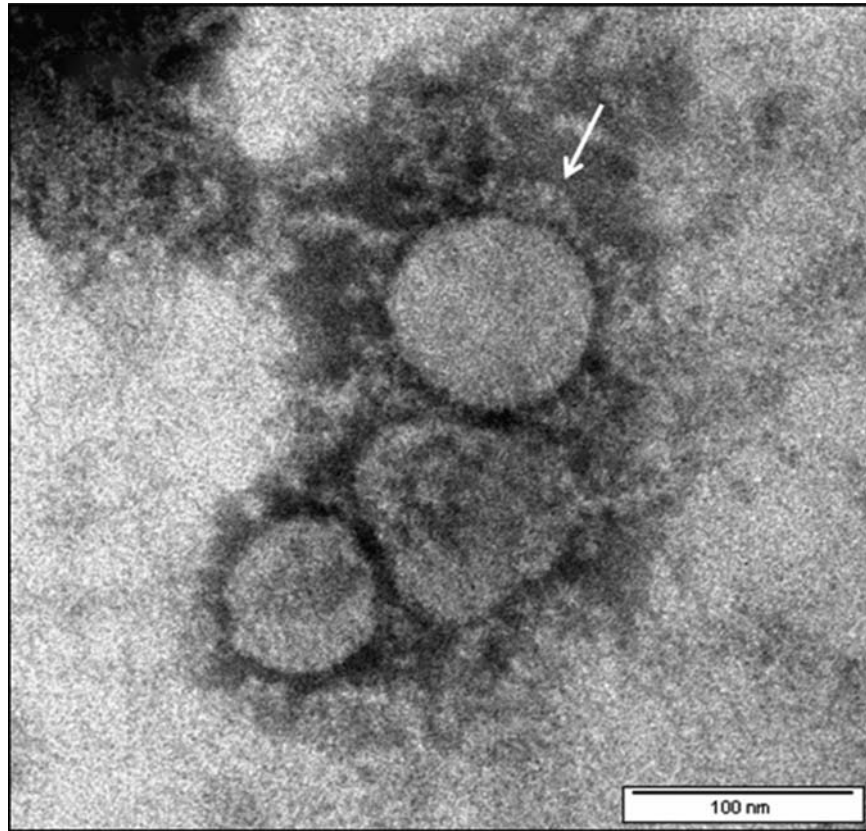


Fig. 1. NCEM of purified FCoV UPM11C/08 showing virion of spherical shapes. The virus particles are surrounded by knob-like spikes envelope (arrow). Scale bar, 100 nm.

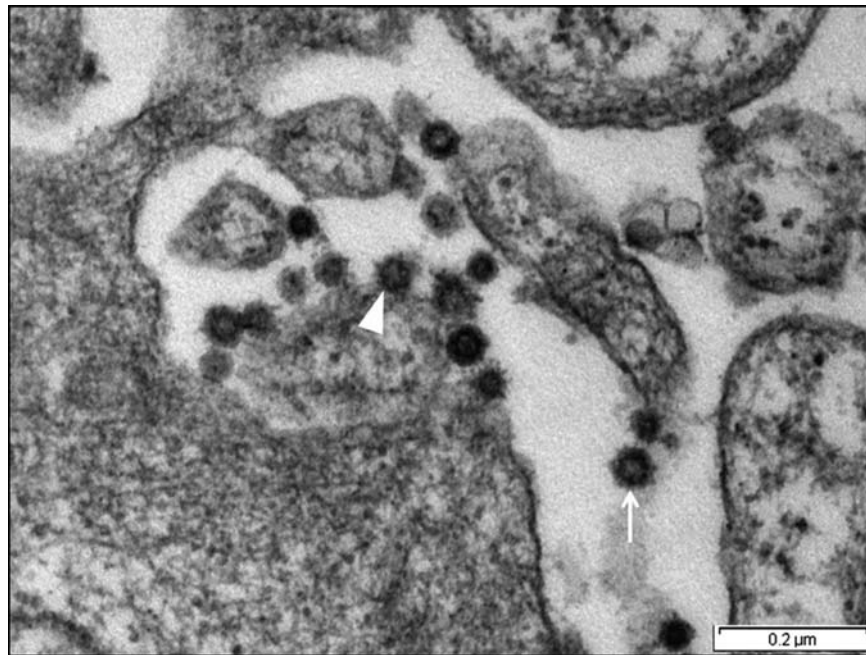


Fig. 2. Micrograph shows Fcwf-4 cell culture infected with FCoV UPM11C/08 at 15 h pi. Virus particles are present at the extracellular compartment and exhibit spherical shaped with spike-like electron-dense envelope (arrow). Virus particles are closely apposed to the plasma membrane (arrowhead). Scale bar, 0.2 μm.

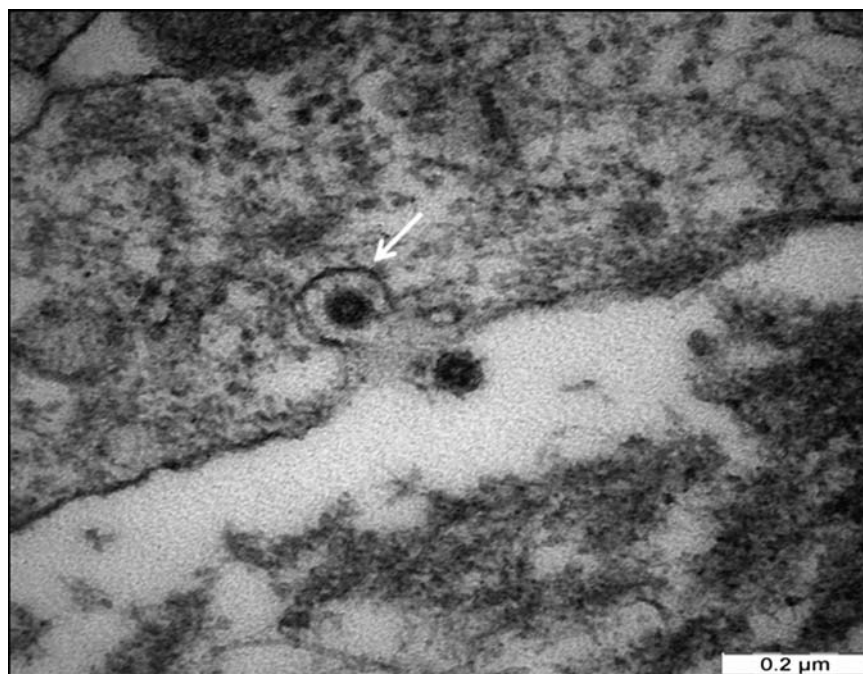


Fig. 3. Micrograph of Fcwf-4 cell culture infected with FCoV UPM11C/08 showing a virus particle invaginating host cell membrane. Note the invaginated virus is coated with a trilaminar membrane (arrow). Scale bar, 0.2 μm .

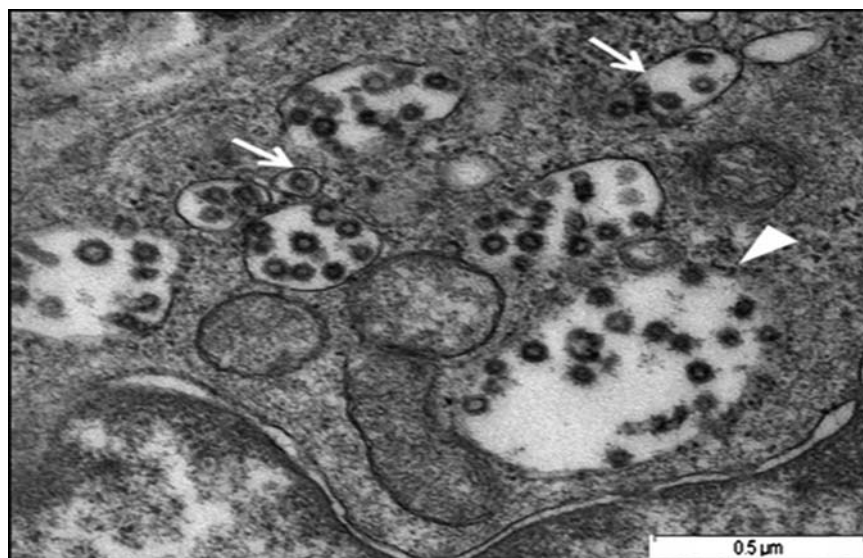


Fig. 4. Micrograph shows small vacuoles containing 1–5 virus-like particles (arrows), while larger ones containing 20–24 virus-like particles (arrowhead) following infection with FCoV UPM11C/08 isolate. Scale bar, 0.5 μm .

abundance while at 48 h pi, the virus particles were detected both at extracellular and intracellular. In many of the instances, the virus particles were closely apposed to the plasma membrane, while few particles were observed to invaginate the cell membrane at different depths into the cytoplasmic

matrix. Deeply invaginated virus particles were seen to carry along with it part of the cell membrane that it invaginates with the absence of the plasma membrane at the site of invagination. Beesley and Hitchcock [21] and many other investigators had reported similar observations but were

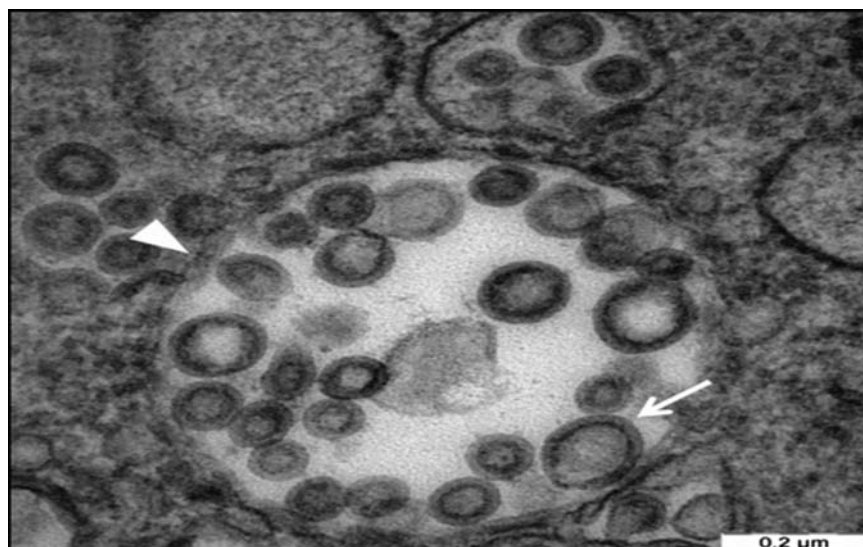


Fig. 5. Micrograph showing the virus-like particles inside a vacuole following infection of FCoV UPM 11C/08 on Fcwf-4 cell culture. Note the smooth electron-dense envelope virus-like particle (arrow) and distinct rounded, firm and thick vacuole membrane (arrowhead). Scale bar, 0.2 μm .

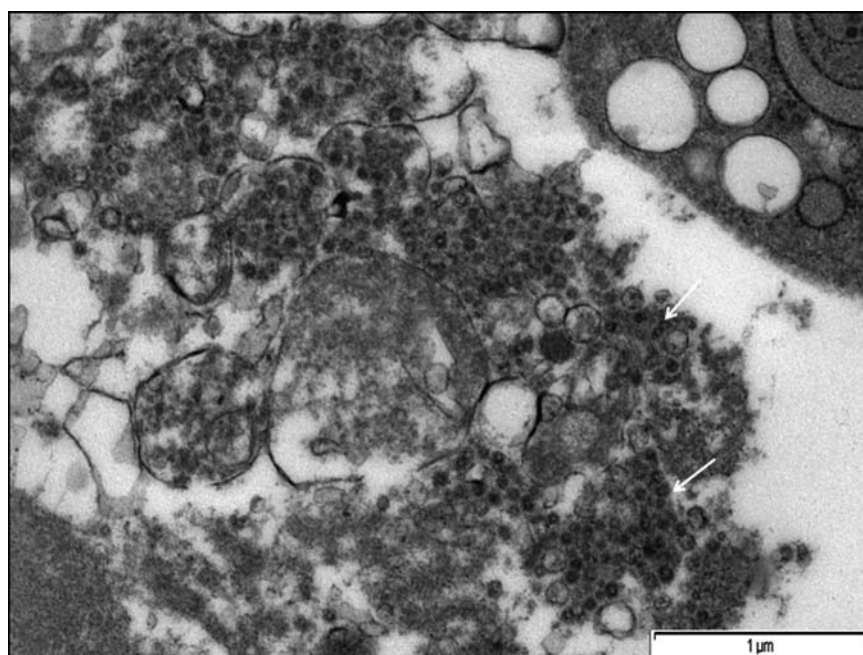


Fig. 6. Micrograph showing aggregation of virus particles within vacuoles following infection of FCoV UPM11C/08 isolate on Fcwf-4 cell culture. Some parts of the vacuoles membrane were no longer intact and leading to spillage of virus-like particles into cytoplasmic matrix (arrows). Scale bar, 1 μm .

of the opinion that invagination of the virus particles could represent a route of secondary infection.

The new insight on the virus particles referred to in the present study was that virus-like particles were present in vacuoles of two types. In addition, the study also showed that the virus particles

appeared in two forms. Both types of vacuoles contained a variable number of particles, ranging from a single to numerous particles. The rough, spike-like electron-dense virus particles present extracellularly and those that invaginated the host cell membrane appeared morphologically similar. At this juncture, it is tempting to postulate the

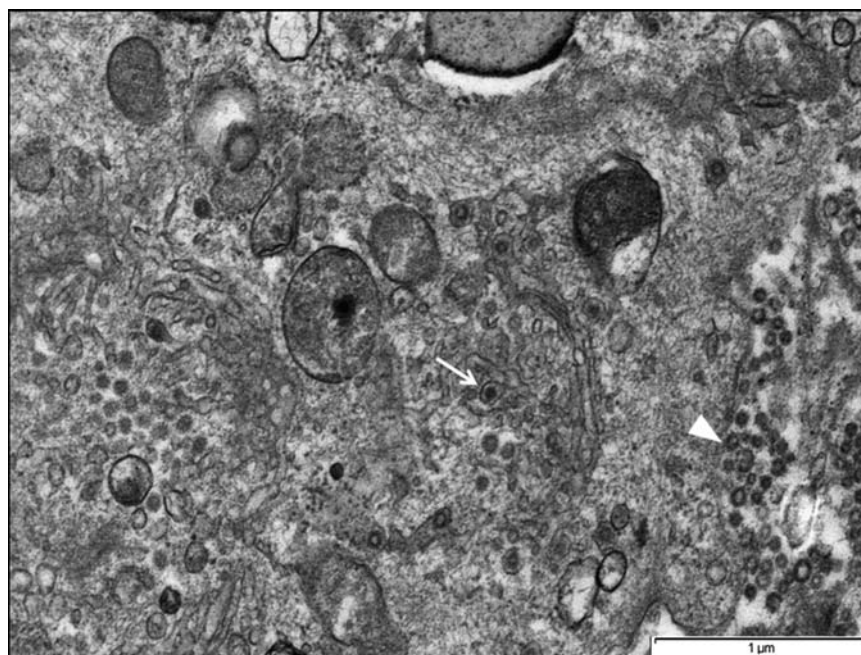


Fig. 7. Micrograph showing virus-like particles in the vesicle of Golgi apparatus (arrow) and aggregations of extracellular virus-like particles (arrowhead) following infection of FCoV UPM11C/08 isolate on Fcwf-4 cell culture. Scale bar, 1 μ m.

possibility that the extracellular particles and those that invaginated the cell membrane were the same viruses present within the vacuoles based on their similar morphological features. However, contrary to many published reports pertaining to the replication and budding of the FCoV particles [20, 21, 27–29], no such proliferative growth involving the vacuolar membrane was reported.

A smooth enveloped electron-opaque virus-like particle detected in this study was found to accumulate in a distinct rounded, firm and thicker vacuole. Similarly, there is no evidence of replication and budding of virus from this vacuole's membrane. We believed that the two morphologically different virus-like particles observed in this study are in fact FCoV as at this juncture of study we are not able to show the transformation between these two distinct particles. Probably, the sizes reflect different maturation stages of the virus particles. Further, the significance of the two types of vacuoles with structurally different virus particles contained is also not known. In this context, it is again tempting to postulate whether the artificial environment and the use of Fcwf-4 cell cultures could induce the formation of two different vacuoles containing two distinct particles. Somewhat similar vacuoles containing virus particles have been noted

in reports by previous workers [14, 20, 28, 30], but these authors provided neither the structural details of these vacuoles nor the virus particles they contained.

In both types of vacuoles observed in the present study, there were clear evidences to indicate the vacuole membrane did not remain intact as spillage of the virus was detected in the cytoplasmic matrix. Thus, apart from the presence of virus particles within vacuoles, the particles were also present freely in the cytoplasmic matrix. When clusters of the particles were present in the vicinity of the Golgi complex, single particle was also present in the vesicle of the Golgi apparatus.

Conclusion

It is concluded from the present study that following the infection of FCoV in Fcwf-4 cell culture, two different morphologically virus-like particles were seen in their respective vacuoles. The vacuoles could be the site for virus replication although no evidence of budding from the vacuolar membrane was observed in this study. Rupture of vacuoles led to the spillage of the virus-like particles into the cytoplasmic matrix.

Funding

This work was supported by the Ministry of Science, Technology and Innovation (MOSTI), Malaysia, project number 02-01-04-SF0485: Development of a rapid test for diagnosis of FCoV.

Acknowledgements

The authors would like to thank the staff of the Imaging Unit, Institute of Bioscience, UPM.

References

- 1 Rohrbach B W, Legendre A M, Baldwin C A, Lein D H, Reed W M, and Wilson R B (2001) Epidemiology of feline infectious peritonitis among cats examined at veterinary medical teaching hospitals. *J. Am. Vet. Med. Assoc.* **218**: 1111–1115.
- 2 Pedersen N C (1995) An overview of feline enteric coronavirus and infectious peritonitis virus infections. *Feline Pract.* **23**: 7–22.
- 3 Addie D D and Jarrett O (1992) A study of naturally occurring feline coronavirus infections in kittens. *Vet. Rec.* **130**: 133–137.
- 4 Pringle C (1999) Virus taxonomy—1999. *Arch. Virol.* **144**: 421–429.
- 5 Cavanagh D (1997) *Nidovirales*: a new order comprising *Coronaviridae* and *Arteriviridae*. *Arch. Virol.* **142**: 629–633.
- 6 Holzworth J E (1963) Some important disorders of cats. *Cornell Vet.* **53**: 157–160.
- 7 Wong W T, Cheng B Y, and Lee J Y S (1983) Feline infectious peritonitis – two case reports. *Kajian Vet. Malaysia* **15**: 30–35.
- 8 Pedersen N C, Boyle J F, Floyd K, Fudge A, and Barker J (1981) An enteric coronavirus infection of cats and its relationship to feline infectious peritonitis. *Am. J. Vet. Res.* **42**: 368–377.
- 9 Ward B C and Pedersen N C (1969) Infectious peritonitis in cats. *J. Am. Vet. Med. Assoc.* **1**: 26–35.
- 10 Addie D D, Toth S, Murray G D, and Jarrett O (1995) Risk of feline infectious peritonitis in cats naturally infected with feline coronavirus. *Am. J. Vet. Res.* **56**: 429–434.
- 11 Arshad S-S, Lee W W, Hassan L, Kamarudin A I M, Siti-Farawahida A W, and Cheng N A B Y (2004) Serological survey of catteries for cats infected with feline coronavirus. *J. Vet. Malaysia* **17**: 19–22.
- 12 Pedersen N C, Black J W, Boyle J F, Evermann J F, McKeirnan A J, and Ott R L (1984) Pathogenic differences between various feline coronavirus isolates. *Adv. Exp. Med. Biol.* **173**: 365–380.
- 13 Motokawa K, Hohdatsu T, Aizawa C, Koyama H, and Hashimoto H (1995) Molecular cloning and sequence determination of the peplomer protein gene of feline infectious peritonitis virus type I. *Arch. Virol.* **140**: 469–480.
- 14 Lai M and Cavanagh D (1997) The molecular biology of corona virus. *Adv. Virus. Res.* **48**: 1–100.
- 15 Pedersen N C, Evermann J F, McKeirnan A J, and Ott R L (1984) Pathogenicity studies of feline coronavirus isolates 79-1146 and 79-1683. *Am. J. Vet. Res.* **45**: 2580–2585.
- 16 Holmes K V and Lai M (1996) *Coronaviridae: the viruses and their replication*. *Fields Virology*, 3rd edn., pp: 1075–1093 (Lippincott-Raven Publishers, Philadelphia, PA).
- 17 Pedersen N C (1987) Virologic and immunologic aspects of feline infectious peritonitis virus infection. *Adv. Med. Biol.* **218**: 529–550.
- 18 Jacobse-Geels H E and Horzinek M C (1983) Expression of feline infectious peritonitis coronavirus antigens on the surface of feline macrophage-like cells. *J. Gen. Virol.* **64**: 1859–1866.
- 19 Mohandas D V and Dales S (1991) Endosomal association of a protein phosphatase with high dephosphorylating activity against a coronavirus nucleocapsid protein. *FEBS Lett.* **282**: 419–424.
- 20 Pedersen N C (1976) Morphologic and physical characteristics of feline infectious peritonitis virus and its growth in autochthonous peritoneal cell cultures. *Am. J. Vet. Res.* **37**: 567–572.
- 21 Beesley J E and Hitchcock L J (1982) The ultrastructure of feline infectious peritonitis virus in feline embryonic lung cells. *J. Gen. Virol.* **59**: 23–28.
- 22 Sharif S, Arshad S-S, Bejo M-H, Omar A A, Zeenathul N, and Hafidz M A (2009) Prevalence of feline coronavirus in two cat populations in Malaysia. *J. Feline Med. Surg.* **11**: 1031–1034.
- 23 Gelderblom H, Renz H, and Özel M (1991) Negative staining in diagnostic virology. *Micron Microsc. Acta* **22**: 435–447.
- 24 Hayat M A (1986) *Basic techniques for transmission electron microscopy* (Academic Press, New York).
- 25 Reynolds E S (1963) The use of lead citrate at high pH as an electron-opaque stain in electron microscopy. *J. Cell. Biol.* **4**: 208–212.
- 26 Hoshino Y and Scott F W (1980) Immunofluorescent and electron microscopic studies of feline small intestinal organ cultures infected with feline infectious peritonitis virus. *Am. J. Vet. Res.* **41**: 672–681.
- 27 Weiss R C and Scott F W (1981) Pathogenesis of feline infectious peritonitis: nature and development of viremia. *Am. J. Vet. Res.* **42**: 382–390.
- 28 Ward J M (1970) Morphogenesis of a virus in cats with experimental feline infectious peritonitis. *Virology* **41**: 191–194.
- 29 Evermann J F, Heeney J L, McKeirnan A J, and O'Brien S J (1989) Comparative features of a coronavirus isolated from a cheetah with feline infectious peritonitis. *Virus. Res.* **13**: 15–27.
- 30 Klumperman J, Locker J K, Meijer A, Horzinek M C, Geuze H J, and Rottier P J M (1994) Coronavirus M proteins accumulate in the Golgi complex beyond the site of virion budding. *J. Virol.* **68**: 6523–6534.